Fourfold Basal Plane Anisotropy of the Nonlocal Magnetization of YNi_2B_2C

L. Civale,[1] A. V. Silhanek,[1] J. R. Thompson,[2,3] K. J. Song,[3] C. V. Tomy,[4] and D. McK. Paul[4]
[1]*Comisión Nacional de Energía Atómica-Centro Atómico Bariloche, 8400 Bariloche, Argentina*
[2]*Oak Ridge National Laboratory, Oak Ridge, Tennessee 37831-6061*
[3]*Department of Physics, University of Tennessee, Knoxville, Tennessee 37996-1200*
[4]*Department of Physics, University of Warwick, Coventry, CV4 7AL, United Kingdom*
(Received 8 July 1999)

Studies of single crystal YNi_2B_2C have revealed a fourfold anisotropy of the equilibrium magnetization in the square crystallographic basal plane. This $\pi/2$ periodicity occurs deep in the superconductive mixed state. In this crystal symmetry, an ordinary superconductive mass anisotropy (as in usual London theory) allows only a constant, isotropic response. In contrast, the experimental results are well described by generalized London theory incorporating nonlocal electrodynamics, as needed for this clean, intermediate-κ superconductor.

PACS numbers: 74.25.Ha, 74.25.Bt, 74.70.Dd

Borocarbide superconductors have received considerable recent attention, due in part to the interaction between magnetism and superconductivity. A rich superconducting phase diagram, including transitions between hexagonal, rhombohedral, and square vortex lattices, has been observed [1–4]. The existence of vortex lattices with nonhexagonal symmetry has been attributed to nonlocality effects on the superconducting electrodynamics [4,5], which arise from the large electronic mean free path ℓ of these clean superconductors. Geometrically, a vortex directed along the tetragonal c axis has squarelike current contours [6]. It has been shown [7] in the nonmagnetic borocarbide YNi_2B_2C that the deviations from the standard (local) London magnetic field dependence of the equilibrium magnetization $M_{\rm eq} \propto \ln(H)$ can be quantitatively accounted for by introducing nonlocal electrodynamics into the London model [8]. Traditionally, it was widely thought that nonlocality effects should be significant only in materials with a Ginzburg-Landau parameter $\kappa = \lambda/\xi \sim 1$, where λ is the London penetration depth and ξ is the superconducting coherence length [9]. Those materials, e.g., Nb, were clean enough to have $\ell \gg \xi$, but the large vortex cores with $\xi \approx \lambda$ make theoretical analysis very difficult. With the development of clean intermetallics and compounds, e.g., YNi_2B_2C where $\kappa \approx 10-15$, core effects are much smaller. Thus a more tractable nonlocal London formalism has been recently developed [8] for understanding these intermediate-to-high κ materials.

In the local London model of superconducting vortices, the material anisotropy is introduced via a second rank mass tensor m_{ij}. In tetragonal materials such as YNi_2B_2C or $LuNi_2B_2C$, the masses in both principal directions in the square basal plane are the same, $m_a = m_b$; thus the superconducting properties are isotropic in the a-b plane. In contrast, nonlocal corrections are expected to introduce [10] a fourfold anisotropy as a function of the magnetic field orientation within the a-b plane. A temperature-dependent in-plane anisotropy of the upper critical field H_{c2} has been observed [11] in the nonmagnetic borocarbide $LuNi_2B_2C$ and described within a Ginzburg-Landau framework incorporating nonlocal effects. However, a direct observation of the in-plane anisotropy deep in the superconducting phase, where the nonlocal London model applies and unusual vortex lattices are observed, has not been reported until now.

In this Letter we show that, in the superconducting mixed state of YNi_2B_2C, the reversible magnetization oscillates with a $\pi/2$ periodicity when the applied field is rotated within the a-b plane. The amplitude of the angular oscillation decreases with field, passes through zero, and then *reverses sign* at a field well below H_{c2}. The results are in good quantitative agreement with the nonlocal London description introduced by Kogan *et al.* [8].

The 17 mg single crystal of YNi_2B_2C investigated in this study is the same as that previously used by Song *et al.* [7] to explore the magnetic response when the applied field $\mathbf{H}$ is parallel to the c axis. The critical temperature is $T_c = 14.5$ K, defined as the point at which the linearly varying magnetization $M(T)$ extrapolates to zero; this ignores a slight "tail" extending to 15.6 K. The crystal is a slab of thickness $t \sim 0.5$ mm, whose shape and size in the basal plane are sketched in Fig. 1. It will be useful to approximate such a shape by an ellipse of axes L_x and L_y. X-ray diffraction shows that the crystallographic c axis is normal to the slab, and the two equivalent (110) axes of the tetragonal structure very approximately coincide with the axes of the ellipse.

Measurements were performed in a Quantum Design SQUID magnetometer with a 50 kOe magnet. Two sets of detection coils allow us to measure both the longitudinal (parallel to $\mathbf{H}$) and transverse (perpendicular to $\mathbf{H}$) components of the magnetization vector $\mathbf{M}$, but only the longitudinal component (denoted hereafter as simply the magnetization M) will be discussed in this Letter. The crystal was mounted into a previously described [12], homemade rotating sample holder with the rotation axis perpendicular to $\mathbf{H}$. The c axis was aligned with the rotation axis, so that $\mathbf{H}$ could be rotated within the basal plane.

 0031-9007/99/83(19)/3920(4)$15.00

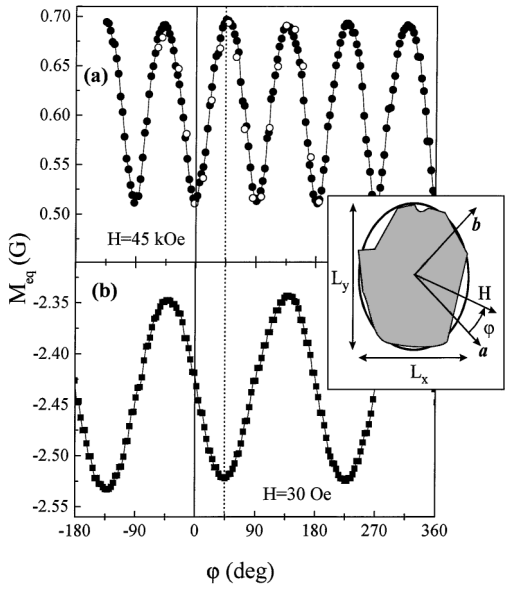

FIG. 1. Equilibrium magnetization $M_{\rm eq}$ at $T = 7$ K, as a function of the angle φ between the applied field **H** (contained in the a-b plane) and the a axis, for (a) $H = 45$ kOe and (b) $H = 30$ Oe. The inset shows a sketch of the crystal shape and crystallographic orientation in the basal plane, superimposed to an ellipse with the same demagnetizing factors.

Figure 1 shows M as a function of the angle φ between **H** and the a axis (see sketch in Fig. 1), at $T = 7$ K and two values of H. The crystal was initially cooled in zero field, H was then applied, and the sample was subsequently rotated in steps of $\Delta\varphi \approx 3.1°$. Each data point was taken at fixed φ.

We first discuss the low field curve of Fig. 1b. As $H = 30$ Oe is well below the lower critical field H_{c1} for all φ, this curve represents the total flux exclusion of the Meissner state. The oscillatory behavior with periodicity π (twofold symmetry) originates from purely geometrical effects. Indeed, a field applied at any orientation within the basal plane can be decomposed in $H_x = H\cos(\varphi + 45°)$ and $H_y = H\sin(\varphi + 45°)$. If we approximate the crystal shape by the ellipse, the Meissner response associated with each component is $4\pi M_i = -H_i/(1 - \nu_i)$, where $i = x; y$, and $\nu_i = t/L_i$ are the demagnetizing factors; thus $4\pi M = -H[\cos^2(\varphi + 45°)/(1 - \nu_x) + \sin^2(\varphi + 45°)/(1 - \nu_y)]$. The best fit to this expression gives $\nu_x \sim 1/4$ and $\nu_y \sim 1/5$. This corresponds to the ellipse of axes $L_x \sim 2.0$ mm and $L_y \sim 2.5$ mm shown in the sketch of Fig. 1.

We now turn to the high field data of Fig. 1a. The applied field, $H = 45$ kOe, is well above $H_{c2} \sim 35$ kOe at this temperature (which is only weakly φ dependent, see below); thus in this case $M(\varphi) = M^{\rm ns}(\varphi)$ is the normal state paramagnetic response. We again observe an oscillatory behavior, but in this case the periodicity is $\pi/2$. By combining the information provided by the x rays with the geometrical effects on the Meissner response, we conclude that the maximum normal state magnetization occurs at the crystallographic orientations $\langle 110\rangle$ and $\langle \bar{1}10\rangle$, while the minimum corresponds to $\langle 100\rangle$ and $\langle 010\rangle$. No hint of the geometry-originated twofold symmetry is observed. This is to be expected, as demagnetizing effects vanish in the limit $|M/H| \ll 1$. Further analysis of $M^{\rm ns}$ suggests that it arises from a low concentration, $\sim$0.001 molar fraction, of rare earth ions, most likely from impurities in the yttrium starting metal. As shown below, $M^{\rm ns}$ is much smaller than the superconducting contribution, except close to H_{c2}.

The above procedure cannot be used in the superconducting mixed state, due to the appearance of magnetic hysteresis arising from vortex pinning. The critical current density J_c is very small in this crystal [7]. As a result, the magnetic hysteresis $(M^{\downarrow} - M^{\uparrow}) \propto J_c$, where $M^{\downarrow}$ and $M^{\uparrow}$ are, respectively, the magnetizations measured in the field-decreasing and field-increasing branches of an isothermal $M(H)$ loop, is small as compared to the equilibrium or reversible magnetization, $M_{\rm eq} \approx (M^{\downarrow} + M^{\uparrow})/2$. In spite of this, the residual hysteresis strongly affects the response obtained by rotating the crystal at fixed T and H, by superimposing a periodicity π (related to shape effects on the critical state magnetization) that almost completely hides the intrinsic $\pi/2$ periodicity of fundamental interest.

To solve this difficulty, we performed magnetization loops at $T = 7$ K at a set of fixed angles and then calculated $M_{\rm eq}(H)$ for each φ. In all cases we extended the loops up to $H = 50$ kOe; thus we could repeat the measurement of $M^{\rm ns}$ in the normal state and compare the data with those obtained by rotating at fixed H. Because of the absence of hysteresis, both determinations of $M^{\rm ns}(H, \varphi)$ should coincide. This is indeed the case, as seen in Fig. 1a, where the open circles represent the data at $H = 45$ kOe obtained from the $M(H)$ loops.

Figure 2 shows $M_{\rm eq}$ (obtained from averaging $M^{\downarrow}$ and $M^{\uparrow}$) as a function of φ for several H. All of the data have the same scale, but the curves at different H have been vertically shifted to accommodate the whole field range within the plot. For $H < 1.5$ kOe, the irreversibility becomes large enough to introduce a significant uncertainty in the determination of $M_{\rm eq}$; consequently, those data have been disregarded. It is apparent that a fourfold symmetry exists in the whole field range of the measurements. To quantify the amplitude of the oscillations, we fitted the curves by $M_{\rm eq}(H, \varphi) = \langle M_{\rm eq}\rangle + \delta M_{\rm eq}(H)\cos(4\varphi)$.

The oscillation amplitudes $\delta M_{\rm eq}(H)$ so obtained are plotted in Fig. 3, while the values of $\langle M_{\rm eq}\rangle(H)$ are shown in the inset. A remarkable fact, clearly visible in Figs. 2 and 3, is that $\delta M_{\rm eq}(H)$ crosses zero and *it reverses sign* at some intermediate field ($\sim$12 kOe) well within the superconducting mixed state. Another interesting observation is that the amplitude of the oscillations at $H \sim 1.5$–2 kOe is as large as that at $H \sim 50$ kOe.

The above results show that a $\pi/2$ basal plane anisotropy exists both in the normal and in the superconducting states. It is also clear from Fig. 3 that a change in the behavior of $\delta M_{\rm eq}(H)$ takes place at the superconducting transition at $H_{c2} \sim 35$ kOe. This observation, together

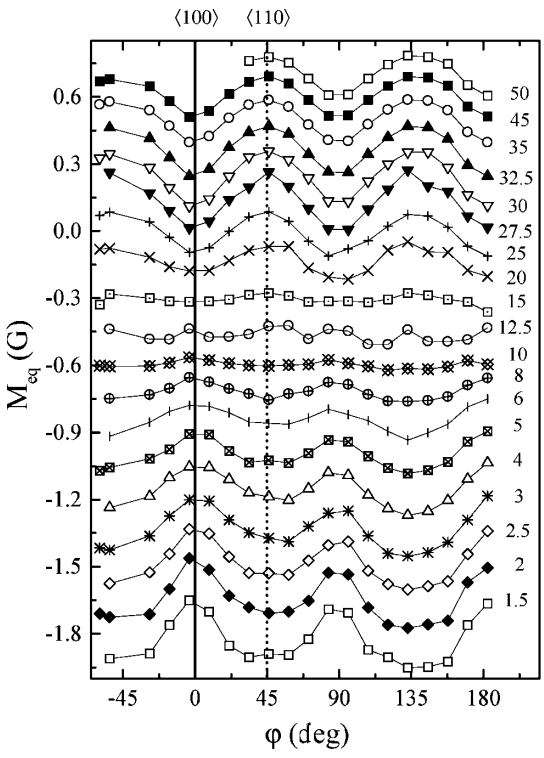

FIG. 2. Reversible magnetization $M_{\rm eq}$ at $T = 7$ K, as a function of the angle φ between the applied field **H** (contained in the *a*-*b* plane) and the *a* axis. The fields (in kOe) are indicated next to each curve. The scale is the same for all of the curves, but data at different H have been vertically shifted.

with the sign reversal and the large amplitudes at low fields, points to the existence of a second source of in-plane anisotropy that, in addition to the normal state one, turns on in the superconducting phase.

Prior to analyzing the superconducting basal-plane anisotropy it is necessary to subtract the normal state contribution, which persists within the superconducting phase. To that end we performed rotations at fixed H, as those shown in Fig. 1a, at several T and H above $H_{c2}(T)$. We found a paramagnetic response that exhibits a fourfold symmetry, with the minimum at $\varphi = 0$ in all cases, i.e., $M^{\rm ns}(\varphi = 45°) > M^{\rm ns}(\varphi = 0°) > 0$ for all T and H. We thus have a well-defined set of data $\delta M^{\rm ns}(H,T)$ which exhibits no sign reversal. The extrapolation is not obvious, however, as $\delta M^{\rm ns}$ is not linear in H. Figure 4 shows all of the $\delta M^{\rm ns}$ data collected at various temperatures $5 \le T \le 16$ K and $H \le 50$ kOe, as a function of H/T. We found that, when plotted in this way, all of the data points collapse on a single curve.

The dotted line in Fig. 4 is a fit to the $\delta M^{\rm ns}(H/T)$ data. The same fit, for the case of $T = 7$ K, is also shown as a dotted line in Fig. 3. We can now subtract that curve from the total $\delta M_{\rm eq}$ shown in Fig. 3, to isolate the superconducting contribution $\delta M^{\rm sc}_{\rm eq}$. Note that, as $\delta M^{\rm ns}$ is always positive and increases monotonically with H, both the sign reversal and the nonmonotonic behavior immediately below H_{c2} exhibited by $\delta M_{\rm eq}$ must arise from the $\delta M^{\rm sc}_{\rm eq}$ contribution.

We now show that the fourfold symmetry of $M^{\rm sc}_{\rm eq}$, as well as the field dependence of $\delta M^{\rm sc}_{\rm eq}$, can be well described using the nonlocal modifications to the London electrodynamics introduced by Kogan *et al.* [8]. According to that model, for $H_{c1} \ll H \ll H_{c2}$,

$$M^{\rm sc}_{\rm eq} = -M_0\left[\ln\left(\frac{H_0}{H} + 1\right) - \frac{H_0}{H_0 + H} + \zeta\right]. \quad (1)$$

Here $M_0 = \Phi_0/32\pi^2\lambda^2$, the new characteristic field $H_0 = \Phi_0/4\pi^2\rho^2$ is related to the nonlocality radius ρ, and $\zeta = \eta_1 - \ln(H_0/\eta_2 H_{c2} + 1)$, where η_1 and η_2 are constants of order unity.

Song *et al.* [7] have shown that the magnetization of this same crystal is very well described by Kogan's model,

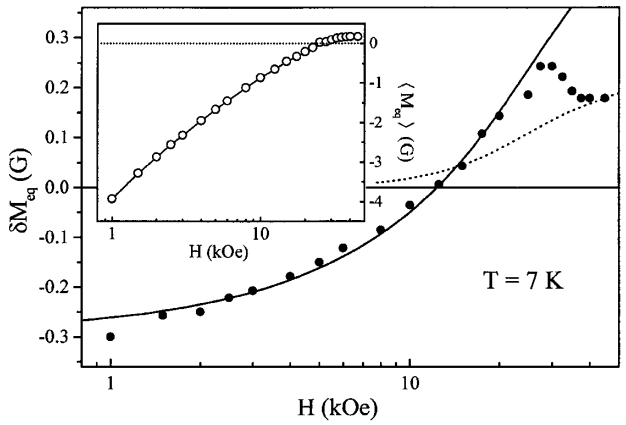

FIG. 3. Amplitude $\delta M_{\rm eq}$ of the fourfold oscillations of the basal plane magnetization, as a function of the applied field H. The dotted line is the normal state contribution $\delta M^{\rm ns}$ obtained from the fit shown in Fig. 4. The solid line is the fit to $\delta M^{\rm sc}_{\rm eq} + \delta M^{\rm ns}$ using Eq. (2) with ϵ_1 as the only fitting parameter. Inset: Average in-plane magnetization $\langle M_{\rm eq}\rangle$, as a function of applied field (see text).

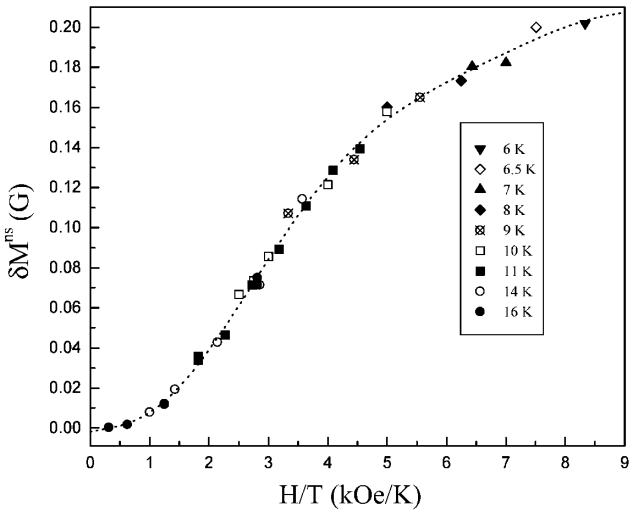

FIG. 4. Amplitude $\delta M^{\rm ns}$ of the fourfold oscillations of the basal plane magnetization in the normal state, as a function of H/T. The dotted line is a polynomial fit.

when $H \parallel c$-axis. A fingerprint of the nonlocality effects is the deviation from the $M_{\rm eq} \propto \ln(H)$ behavior predicted by the local London model. The curvature clearly visible in the inset of Fig. 3 is thus a strong indication that nonlocality also plays a major role when $H \perp c$-axis. It is worth mentioning that, although a quantitative analysis of the curve in the inset of Fig. 3 in terms of Eq. (1) would require removal of the normal state magnetization, its contribution is small and would not significantly modify the curvature seen in the $M_{\rm eq}$ vs $\ln(H)$ data.

We now apply Eq. (1) to the analysis of our data. In principle, the basal plane anisotropy could be ascribed to the material parameters M_0, H_0, and H_{c2}. However, $M_0 \propto \lambda^{-2}$ is isotropic within the a-b plane of a tetragonal structure. On the other hand, fourfold variations of H_{c2} within the basal plane have been observed in $LuNi_2B_2C$ and attributed to nonlocality [11]. We then assume that both H_0 and H_{c2} have $\pi/2$ periodicity, $H_0(\varphi) = \langle H_0 \rangle + \delta H_0 \cos(4\varphi)$ and $H_{c2}(\varphi) = \langle H_{c2} \rangle + \delta H_{c2} \cos(4\varphi)$. To first order in δH_0 and δH_{c2} we obtain

$$\delta M_{\rm eq}^{\rm sc} = -M_0 \left[\left(\frac{1}{(1 + \frac{H}{\langle H_0 \rangle})^2} - \alpha \right) \epsilon_1 + \alpha \epsilon_2 \right], \quad (2)$$

where

$$\alpha = \frac{1}{1 + \eta_2 \frac{\langle H_{c2} \rangle}{\langle H_0 \rangle}}; \qquad \epsilon_1 = \frac{\delta H_0}{\langle H_0 \rangle}; \qquad \epsilon_2 = \frac{\delta H_{c2}}{\langle H_{c2} \rangle}.$$

Experimentally, we have determined $\langle H_{c2} \rangle = 35$ kOe and $\delta H_{c2} \sim 0.4$ kOe (at $T = 7$ K), so we can fix $\epsilon_2 = 0.01$. We could also attempt to determine M_0 and $\langle H_0 \rangle$ by fitting our $M_{\rm eq}$ data with Eq. (1). However, this is a difficult task that requires [7] the measurement of a large set of temperatures to check the consistency of the results. Instead, we decided to use the results of Song *et al.* [7] (for $H \parallel c$-axis) as good estimates. For $T = 7$ K, we take $\langle H_0 \rangle = 56$ kOe and $M_0 = 5.2$ G. (Here we scaled down $M_0 \propto 1/\lambda_a \lambda_c$ by the experimental mass anisotropy, $\gamma \approx 1.15$, between the c axis and the a-b plane, which is close to the value $\gamma \sim 1.1$ obtained from band structure calculations [13].) In any case, small variations in any of these parameters will not significantly affect the rest of the analysis. If we also assume $\eta_2 \sim 1$, we obtain $\alpha \sim 2/3$. With these fixed parameters, we fit our $\delta M_{\rm eq}^{\rm sc}(H)$ data with Eq. (2), with the single free parameter ϵ_1. We obtain $\epsilon_1 = 0.14$. The fitted curve (for $\delta M_{\rm eq}^{\rm sc} + \delta M^{\rm ns}$) is shown as a solid line in Fig. 3.

The very good coincidence between our data and the model is remarkable. With a single fitting parameter ϵ_1, which is field independent, we have been able to account for the nontrivial H dependence of $\delta M_{\rm eq}^{\rm sc}$, including the sign reversal at intermediate fields. Of course, the fit deviates from the data close to H_{c2}, where the London model fails. These experimental results show that nonlocality effects have a profound effect on these clean, intermediate-κ superconductors and they underscore the remarkable utility of the generalized London theory.

In summary, we have demonstrated a fourfold anisotropy in the square basal plane of clean single crystal YNi_2B_2C. This superconducting response is inconsistent with conventional local London theory, but it is well explained by a generalized London model incorporating nonlocal electrodynamics, with parameters based largely on complementary experiments. These observed effects of nonlocality persist deep in the superconducting state, where complex, evolving vortex lattices occur.

We are pleased to acknowledge useful discussions with V. G. Kogan. A. V. S. is member of CONICET. Collaboration between UTK and CAB was supported in part by a UTK Faculty Research Fund. Research at the ORNL is supported by the Division of Materials Sciences, U.S. Department of Energy under Contract No. DE-AC05-96OR22464 with Lockheed Martin Energy Research Corporation.

Note added.—While preparing this manuscript, we learned that P. C. Canfield *et al.* at the Ames Laboratory have observed similar oscillations of the basal plane magnetization of $LuNi_2B_2C$.

[1] M. Yethiraj *et al.*, Phys. Rev. Lett. **78**, 4849 (1997).
[2] M. R. Eskildsen *et al.*, Phys. Rev. Lett. **79**, 487 (1997).
[3] D. McK. Paul *et al.*, Phys. Rev. Lett. **80**, 1517 (1998).
[4] Y. De Wilde *et al.*, Phys. Rev. Lett. **78**, 4273 (1997).
[5] V. G. Kogan *et al.*, Phys. Rev. B **55**, R8693 (1997).
[6] M. Yethiraj *et al.*, Phys. Rev. B **58**, R14 767 (1998).
[7] K. J. Song *et al.*, Phys. Rev. B **59**, R6620 (1999).
[8] V. G. Kogan *et al.*, Phys. Rev. B **54**, 12 386 (1996).
[9] See, e.g., *Superconductivity*, edited by R. D. Parks (Marcel Dekker, New York, 1969), p. 37.
[10] V. G. Kogan, P. Miranovic, and D. McK. Paul, in *The Superconducting State in Magnetic Fields: Special Topics and Trends*, edited by C. A. Sa de Melo, Directions in Condensed Matter Physics Vol. 13 (World Scientific, Singapore, 1998).
[11] V. Metlushko *et al.*, Phys. Rev. Lett. **79**, 1738 (1997).
[12] S. Candia and L. Civale, Supercond. Sci. Technol. **12**, 192 (1999); A. Silhanek *et al.*, Phys. Rev. B **59**, 13 620 (1999).
[13] D. J. Singh, Solid State Commun. **98**, 899 (1996).